Andrzej SZELMANOWSKI
Air Force Institute of Technology
ORCID: 0000-0001-6183-0241

Michał BUREK
Polish Air Force University
e-mail: m.burek@law.mil.pl; ORCID: 0000-0002-6862-9644

Piotr ROGALA
1st Airlift Base

Mariusz IZDEBSKI
Warsaw University of Technology
ORCID: 0000-0002-9157-7870

DOI: 10.55676/asi.v4i2.89

OPTIMALISED PHYSICAL MODEL OF INERTIAL NAVIGATION SYSTEM AS EDUCATION SIMULATOR

ZOPTYMALIZOWANY MODEL FIZYCZNY SYSTEMU NAWIGACJI INERCJALNEJ JAKO SYMULATOR EDUKACYJNY

Abstract

This paper presents an educational simulator of an inertial navigation system built at the Air Force Institute of Technology. The article focuses on the presentation of the influence of instrumental errors of measurement elements on the calculation model, using interference simulation methods. Problems of diagnosing inertial navigation system malfunctions were analysed, covering older (gimballed) and modern (non-gimballed) solutions. The theoretical aspects of the performance of these systems are discussed, using matrix calculus and fault diagram. The main part of the paper presents the optimisation of the physical model of the navigation system, focusing on hardware, algorithms, and signal conditioning modules. The simulator demonstration includes the introduction of disturbances and error analysis of various aspects of the system. The summary points out the importance of the simulator test method for training avionics students, flight engineering service and pilots, considering it as an essential part of supporting the educational process in the field of integrated avionics systems.

Keywords: physical model, simulator, inertial navigation system

Streszczenie

W artykule przedstawiono symulator edukacyjny systemu nawigacji inercjalnej zbudowany w Instytucie Technicznym Wojsk Lotniczych. Artykuł skupia się na prezentacji wpływu błędów instrumentalnych elementów pomiarowych na model obliczeń, wykorzystując metody symulacji zakłóceń. Analizowano problemy diagnozowania niesprawności systemów nawigacji inercjalnej, obejmując starsze (kardanowe) i nowoczesne (bezkardanowe) rozwiązania. Omówiono teoretyczne aspekty działania tych systemów, używając rachunku macierzowego i schematu błędów. W głównej części artykułu przedstawiono optymalizację modelu fizycznego systemu nawigacji, skupiając się na sprzęcie, algorytmach i modułach kondycjonowania sygnałów. Demonstracja symulatora obejmuje wprowadzanie zakłóceń i analizę błędów w różnych aspektach systemu. Podsumowanie wskazuje na znaczenie metody badań z użyciem symulatora do szkolenia studentów awioniki, służby inżynieryjno-lotniczej i pilotów, uznając go za istotny element wsparcia procesu edukacyjnego w dziedzinie zintegrowanych systemów awionicznych.

Słowa kluczowe: model fizyczny, symulator, systemy awioniczne

Artykuł wpłynął do redakcji: 28.09.2023 / Zatwierdzono do publikacji: 30.12.2023

1. INTRODUCTION

Inertial navigation, which uses sensors to determine motion parameters and spatial orientation, is crucial for navigation systems. Recent research focuses on various inertial sensors, enhancing navigation through integration with visual systems. Since the 1930s, these systems have evolved significantly, increasing accuracy and reliability.

Research focuses on innovative strategies to increase the accuracy of navigation systems, including the integration of various navigation schemes and improving algorithms to optimize navigation performance. The integration of multiple sensors, such as vision systems and ultrasonic positioning, extends navigational functionality, especially where GPS signals are unreliable[1].

Research efforts also include modeling the performance of navigation systems in both autonomous and integrated modes, and securing laboratory research[2]. Inertial navigation systems are crucial in both military and civilian applications, providing essential navigational information and enhancing operational efficiency. In the military context, integration with advanced technologies, such as Doppler sonar and underwater acoustic positioning systems, is strategically significant[3]. In civilian applications, these systems are invaluable in precision agriculture, automated mining, and onboard Earth observation systems. Advanced calibration and error compensation techniques are crucial for optimizing the performance of navigation systems. Calibration methods, addressing temperature effects on encoders and gyro drift estimation, reduce errors and ensure accurate navigation cardoned. The fusion of information from multiple inertial sensors with an adaptive Kalman filter increases the resilience and accuracy of systems, especially in autonomous vehicles[4].

Inertial navigation continues to evolve, driven by research on sensor technologies, algorithm development, and sensor fusion techniques. Integration with complementary technologies, such as computer vision and artificial intelligence, expands the capabilities of these systems. Despite long-term experience with inertial navigation systems, the Polish Armed Forces still face diagnostic issues due to the technological complexity of these systems. This is confirmed by analyses of malfunctions in both older (gimballed) and modern (non- cardoned) systems used in contemporary aircraft[5].

1 S. Godha, G. Lachapelle, Foot Mounted Inertial System for Pedestrian Navigation, Measurement Science and Technology 19, no. 7 (May 2008): 075202, https://doi.org/10.1088/0957-0233/19/7/075202.

2 J. Mytych, M.J. Ligarski, Expert Assessment of Conditions for Accredited Quality Management System Functioning in Testing Laboratories, Management Systems in Production Engineering 26, no. 1 (March 1, 2018): 42–48, https://doi.org/10.2478/mspe-2018-0007.

3 M. Zieja et al., A Method for the Interpretation of Sonar Data Recorded during Autonomous Underwater Vehicle Missions, Polish Maritime Research 29, no. 3 (September 1, 2022): 176–86, https://doi.org/10.2478/pomr-2022-0038.

4 M. Izdebski, I. Jacyna-Gołda, P. Gołda, Minimisation of the Probability of Serious Road Accidents in the Transport of Dangerous Goods, Reliability Engineering & System Safety 217 (2022): 108093.

5 P. Rogala, Statyczna Metoda Oceny Stanu Technicznego Systemu Nawigacji Inercjalnej, ITWL, Warszawa 2023.

 DOI: 10.55676/asi.v4i2.89

Fig. 1. View of Su-22 aircraft during IKW-8 system diagnostics in military unit conditions
Source: P. Rogala, Statyczna Metoda Oceny..., op. cit.

Synthetic descriptions of navigation system functions form the basis for building simulation models and optimizing them in terms of architecture and software. Work conducted at the Air Force Institute of Technology has resulted in an educational simulator for the inertial navigation system, allowing the testing of navigation algorithms.

In conclusion, inertial navigation systems are essential in both military and civilian technology, providing reliable, autonomous, and precise navigation solutions that significantly contribute to the efficiency and effectiveness of various operations and applications.

2. MODELS OF INERTIAL NAVIGATION SYSTEMS

Initially developed for military applications, inertial navigation systems have evolved significantly, becoming key components of modern technology. Integrating inertial sensors with GNSS has greatly improved navigation accuracy and reliability in both military and civilian contexts[6].

The development of strapdown systems marked a milestone, providing precise navigation for unmanned vehicles and submarines. Innovations in calibration and error compensation, along with advanced algorithms like Kalman and Madgwick filters, have further enhanced their performance. Advancements in MEMS, fibre optic (FOG), and laser (RLG) technologies have made sensors smaller, lighter, and cheaper, enabling mobile navigation solutions. Integrating these systems with visual and AI technologies has expanded their capabilities, making them essential in modern navigation.

Inertial navigation systems are crucial in civil and military aviation, driven by the difficulty of acquiring high-quality systems on the international market, which often requires government approval.

[6] Y. Yang, Y. Song, Y. Zhu, Innovation Research on Strapdown Inertial Navigation Technology, International Journal of Mechatronics and Applied Mechanics 2017 (January 1, 2017): 72–77.

The results of work carried out at the Air Force Institute of Technology, Warsaw University of Technology and the Air Force Academy, among others, have shown that it is possible to develop and build our own physical models. The analytical work carried out, including the development and verification of simulation models, provided the basis for the construction of an educational simulator of an inertial navigation system in the software version of the and physical model[7].

2.1. MATHEMATICAL MODELS

General mathematical models of inertial navigation systems, among which gimbal and non-gimbal systems can be distinguished[8], proved to be the basic data for the construction of the educational simulator.

Aeronautical inertial navigation systems, both gimballed and non-gimballed, are based on measuring the linear accelerations of the aircraft, and integrating them in a suitably selected coordinate system (usually navigation), which allows the determination of the components of travel speed and navigation position. The equation of motion in inertial navigation can be rearranged as[9]:

$$\frac{dv(t)}{dt} = a(t) - [\omega(t)\ x\ \Omega_Z]\ x\ v(t) + \ g_Z \tag{1}$$

where:

$v(t)$ – the vector of the aircraft's cruising speed;
$a(t)$ – vector of aircraft linear acceleration components measured in the assumed platform (gimbal or analytical) system;
$\omega(t)$ – vector of aircraft angular velocity components measured in the assumed platform system (gimbal or analytical);
Ω_Z – vector of angular velocity of the Earth's rotation;
g_Z – vector of Earth acceleration derived from the Earth's gravity.

In a detailed version, the above equation can be written in the form[10], according to which the change in the components of the travel speed is described:

$$\begin{bmatrix} \dot{V}_N \\ \dot{V}_E \\ \dot{V}_V \end{bmatrix} = D_T^B \begin{bmatrix} a_x \\ a_y \\ a_z \end{bmatrix} - \begin{bmatrix} 0 & 2\Omega_Z + \dot{\lambda}sin\varphi & -\dot{\varphi} \\ -2\Omega_Z + \dot{\lambda}sin\varphi & 0 & -2\Omega_Z + \dot{\lambda}cos\varphi \\ \dot{\varphi} & 2\Omega_Z + \dot{\lambda}cos\varphi & 0 \end{bmatrix} \cdot \begin{bmatrix} V_N \\ V_E \\ V_V \end{bmatrix} + \begin{bmatrix} 0 \\ 0 \\ g_Z \end{bmatrix} \tag{2}$$

[7] A. Szelmanowski et al., Optymalizacja Zbudowanego w ITWL Modelu Fizycznego Systemu Nawigacji Zliczeniowej Klasy AHRS/INS w Zakresie Jego Konfiguracji Sprzętowej i Algorytmów Działania, BT ITWL, Warszawa 2021; A. Szelmanowski et al., Symulator Diagnostyczny Dla Systemu Nawigacji Inercjalnej Wykorzystujący Statyczną Metodę Oceny Stanu Technicznego, in XI Konferencja Naukowa Bezpieczeństwa i Niezawodności KONBiN 2022, Piekary Śląskie 2022, 07-10.06.

[8] M. Kayton, W.R. Fried, Avionics Navigation Systems, 2nd Edition, A Wiley-Interscience Publication, 1997.

[9] Z. Gosiewski, A. Ortyl, Algorytmy Inercjalnego Bezkardanowego Systemu Orientacji i Położenia Obiektu o Ruchu Przestrzennym, vol. 12, Awionika, Wyd. Instytutu Lotnictwa, Warszawa 1999.

[10] Ibidem.

 DOI: 10.55676/asi.v4i2.89

$$\begin{bmatrix} \dot{\varphi} \\ \dot{\lambda} \\ \dot{h} \end{bmatrix} = \begin{bmatrix} (R_M + h)^{-1} & 0 & 0 \\ 0 & [(R_N + h)cos\varphi]^{-1} & 0 \\ 0 & 0 & -1 \end{bmatrix} \cdot \begin{bmatrix} V_N \\ V_E \\ V_V \end{bmatrix} \quad (3)$$

where:

V_N, V_E, V_V – components of the aircraft's travel speed vector;

D_T^B – transformation matrix from the measurement system to the navigation system;

λ, φ, h – longitude, latitude and altitude of the aircraft;

a_x, a_y, a_z – components of the aircraft linear acceleration vector;

Ω_Z – components of the aircraft linear acceleration vector;

g_Z – ground acceleration from the Earth's gravity.

The transformation matrix in cardless systems is updated from the measured angular velocities of the aircraft.

2.2. PHYSICAL MODELS OF INERTIAL NAVIGATION SYSTEMS

In the study[11], it is shown that it is convenient to use a static method for analysing the errors of an inertial navigation system under special conditions, in which there are no changes in the actual navigation position and travel speed components (the system measurement module is installed stationary on a rotary table designed to change spatial orientation angles). This method of testing facilitates the determination of the position and travel speed determination errors of the inertial navigation system depending on the selected instrumental errors and enables its technical condition to be assessed.

An example of a gimbal system is the IKW-8 system (Figure 2), operated on Su-22 aircraft, which uses the classic gimbal solution.

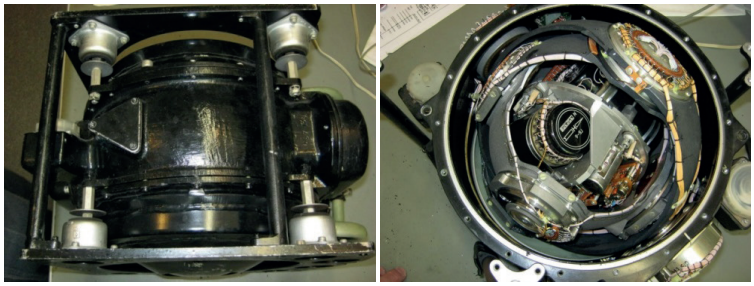

Fig. 2. View of the IKW-8 system (left) and its internal design (right)
Source: P. Rogala, Statyczna Metoda Oceny..., op. cit.

The EGI-3000 system (Figure 3) on W-3PL helicopters uses RLG laser angular velocity sensors and MEMS accelerometers.

11 P. Rogala, Statyczna Metoda Oceny..., op. cit.

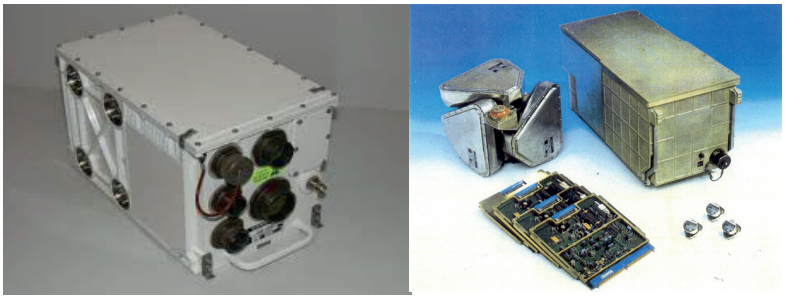

Fig. 3. View of the EGI-3000 system (left) and its internal design (right)
Source: THALES, Functional Specification of Inertial Navigation System TOTEM-3000 / EGI-3000, Bordeaux, France 2010.

2.3. SIMULATION MODELS OF INERTIAL NAVIGATION SYSTEMS

The uncertainty analysis of one channel of the inertial navigation system can use Kayton & Fried's scheme[12]. This allows simplified analysis for short period oscillations, omitting long period oscillations and errors from Coriolis acceleration, Earth's acceleration changes, and diurnal motion velocity changes based on latitude[13].

Based on the diagram taken from Kayton & Fried's schematic diagram, it can be shown that navigational positioning errors for the northern component can be determined as follows:

$$\Delta S_N(t) = \left\{ K_P^S \Delta P + K_\Phi^S \Delta\Phi \right\} \left[1 - \cos(\omega_S t) \right] + \left\{ K_G^S \Delta G + K_\Psi^S \Delta\Psi \right\} \left[t - \sin(\omega_S t) / \omega_S \right] \quad (4)$$

where:

$\Delta S_N(t)$ – north component of the aircraft's navigational position;

K_P^S , K_Φ^S, K_G^S , K_Ψ^S – instrumental uncertainties rates of the inertial navigation system measured in the adopted platform arrangement (gimbal or analytical);

ΔP – instrumental error of the horizontal accelerometer measured in the adopted platform arrangement (gimbal or analytical);

ΔG – instrumental uncertainties of the horizontal gyroscope measured in the adopted platform arrangement (gimbal or analytical).

Simulation studies have shown that, during aircraft flight, the constant drift of the horizontal gyroscope causes a linearly increasing position error (which is superimposed by oscillations at the Schuler frequency), as well as travel speed and yaw errors, which are also oscillatory at the Schuler frequency. A constant horizontal acceleration error induces only oscillations at the Schuler frequency. These studies have also

12 M. Kayton, W.R. Fried, Avionics Navigation Systems, op. cit.
13 P. Rogala, Statyczna Metoda Oceny..., op. cit.

 DOI: 10.55676/asi.v4i2.89

shown that it is more convenient for the analysis and evaluation of an inertial navigation system to study the effect of instrumental errors on the variation of the travel speed components.

Simulation studies of the scheme have shown that navigation position determination errors for the northern component can be determined as:

$$\Delta V_N(t) = \left\{ K_P^V \Delta P + K_\Phi^V \Delta\Phi \right\} \left[\sin(\omega_S t) \right] + \left\{ K_G^V \Delta G + K_\Psi^V \Delta\Psi \right\} \left[1 - \cos(\omega_S t) \right] \quad (5)$$

where:

$\Delta V_N(t)$ – the northern component of the aircraft's cruising speed;

K_P^V , K_Φ^V, K_G^V , K_Ψ^V – instrumental uncertainties rates of the inertial navigation system measured in the adopted platform arrangement (gimbal or analytical).

Analysis of the results obtained shows that the constant drift of the horizontal gyroscope results in a constant velocity error (which is superimposed by oscillations at the Schuler frequency). The systematic error of the horizontal accelerometer, on the other hand, gives a position error that varies harmonically (Schuler frequency oscillations). Errors in the introduction of initial conditions (position, velocity and deviation from vertical result in position errors of an of an oscillatory nature with a limited value).

According to[14], error analysis of inertial navigation systems can be effective for short periods of their operation (less than 4 hours of operation) and at high airspeeds (of the order of 0.3 < Ma < 4), with the Schuler frequency being dominant. Angular velocity error waveforms contain oscillations called Schuler oscillations[15]. For longer periods of their operation (well above 4 hours of operation) and at low flight speeds (Ma of the order of 0.3) the dominant frequency is related to the angular velocity of the Earth's diurnal motion.

In addition, a shortcoming of the available mathematical descriptions is that the errors presented in[16] only apply to position determination and in one navigation channel (north). Using the indications given in the literature, among others[17], it was assumed that a mathematical description of the travel speed errors, respectively for its northern and eastern components, respectively, due to the cyclical nature of their variations.

3. EDUCATIONAL SIMULATOR OF THE INERTIAL NAVIGATION SYSTEM

Using dependencies (2) and (3), a simulation model of the inertial navigation system was developed in the Matlab-Simulink package. This model is the main computational

14 M. Kayton, W.R. Fried, Avionics Navigation Systems, op. cit.

15 P.G. Savage, Strapdown Inertial Navigation Integration Algorithm Design Part 1, Attitude Algorithms, Journal of Guidance, Control and Dynamics 21, no. 1, 1998.

16 M. Kayton, W.R. Fried, Avionics Navigation Systems, op. cit.

17 P. Rogala, Statyczna Metoda Oceny..., op. cit.; A. Szelmanowski et al., Symulator Diagnostyczny..., op. cit.; A. Szelmanowski et al., Optymalizacja Zbudowanego w ITWL..., op. cit.

element of an educational simulator designed to determine and visualize the course of navigation parameter errors in the inertial navigation system.

The simulation model schematic in Matlab-Simulink presents input data and their processing in a central block labeled «KOD.» The input data includes:

1. DPX [m/s²] – with a value of 0.00001.
2. DPY [m/s²] – with a value of 0.00001.
3. DGX [deg/h] – with a value of 0.01.
4. DGY [deg/h] – with a value of 0.01.
5. DTETA [deg] – with a value of 0.01.
6. DGAMA [deg] – with a value of 0.01.
7. DPSI [deg] – with a value of 0.01.
8. DFI [deg] – with a value of 0.01.
9. PSI [deg] – with a value of 90.

These input data are transferred to the central computational block, which processes them to obtain two main results:

1. DVN – north component of travel speed.
2. DVE – east component of travel speed.

These results are then displayed on a monitor labeled «PRZEB.»

The constructed simulation model allows for the input of data and processing of this data by an appropriate computational algorithm (with selected signal conditioning modules and preliminary filtering), resulting in the visualization of the error courses of the north component DVN and the east component DVE of travel speed. Additionally, the error courses of navigation position components and spatial orientation angles as the main parameters determined in the inertial navigation system can be visualized.

3.1. SIMULATION MODEL OF AN INERTIAL NAVIGATION SYSTEM SIMULATOR

The simulation model of the inertial navigation system (Figure 4) serves as the primary element of the educational simulator, including measurement paths (accelerometer and gyroscope signals), Coriolis effect considerations, and adjustments for Earth's angular velocity and gravitational acceleration changes.

The DPX block allows for the introduction of linear acceleration sensor signal error in the longitudinal axis of the modeled measurement platform, and the DPY block introduces linear acceleration sensor signal error in the transverse axis of the modeled platform (gyro or analytical for a strapdown system). Similarly, the DGX block allows for the introduction of angular velocity sensor signal error in the longitudinal axis, and the DGY block introduces angular velocity sensor signal error in the transverse axis of the modeled platform. For the aircraft's spatial orientation angles, the DTETA and DGAMA blocks allow for the introduction of leveling system errors (in the pitch and roll channels), while the DPSI block introduces gyrocompass system errors (in the heading channel). Finally, the DFI block allows for the introduction of latitude setting errors, and the PSI block allows for the introduction of the specified heading of the

 DOI: 10.55676/asi.v4i2.89

modeled measurement platform of the inertial navigation system, corresponding to the initial orientation on the KPA-5 tilt table or installed on the aircraft[18].

The KOD block is used to input the code of the tested computational algorithm, depending on the selected scheme. It contains computational modules for the base algorithm and additional modules accounting for changes in linear acceleration resulting from the Coriolis effect, changes in gravitational acceleration values, and changes in Earth's rotational velocity components depending on the current latitude of the aircraft.

The developed simulation model was used for comparative studies of specialized navigation algorithms implemented in the physical model of the dead reckoning navigation system of the AHRS/INS class, built at the Military Aviation Technical Institute.

For partial simulation studies on the aircraft's spatial orientation angles, the computational scheme (Figure 4), developed at the Military Aviation Technical Institute. The main spatial orientation module, which is part of the Matlab-Simulink simulation model of the inertial navigation system, includes detailed modules such as the determination of Euler angles and geographic and magnetic headings.

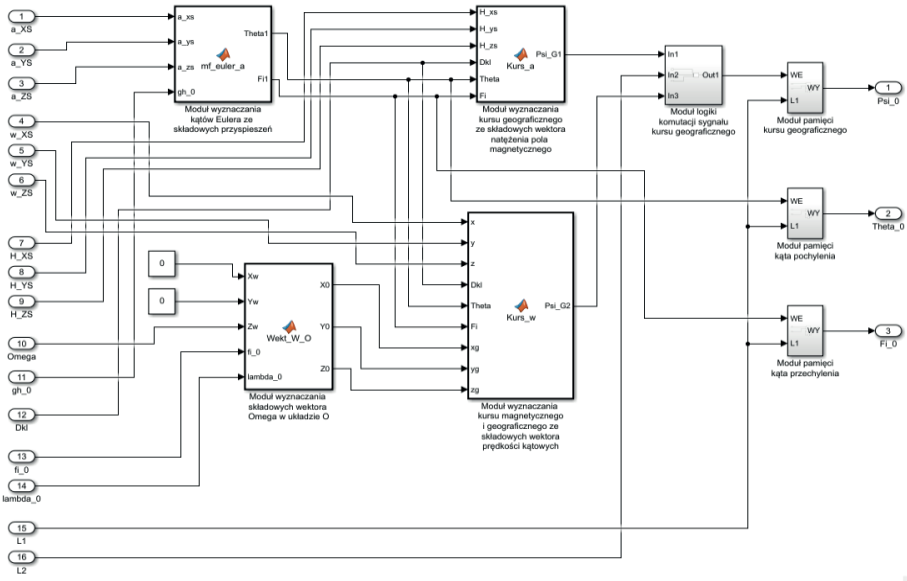

Fig. 4. Diagram of spatial orientation angle calculations in the Matlab-Simulink package

Source: A. Szelmanowski et al., Optymalizacja Zbudowanego w ITWL..., op. cit.

The simulation results presented here, as an example, include selected cases of the impact of isolated errors (for accelerometer and gyroscope mouth bias) occurring in a cardless inertial navigation system.

18 P. Rogala, Statyczna Metoda Oceny..., op. cit.

To illustrate the influence of errors causing sinusoidal travel speed errors, according to the sin(ω_S t) function, modelling results (Figure 5) obtained from the inertial navigation system simulator are presented for selected values of the systematic error of the DPX accelerometer in the longitudinal axis of the aircraft. Analysis of the results showed that the errors only affect either the northern component of the travel speed (when the aircraft is set on a 0° heading) or only the eastern component of the travel speed (when the aircraft is set on a 90° heading).

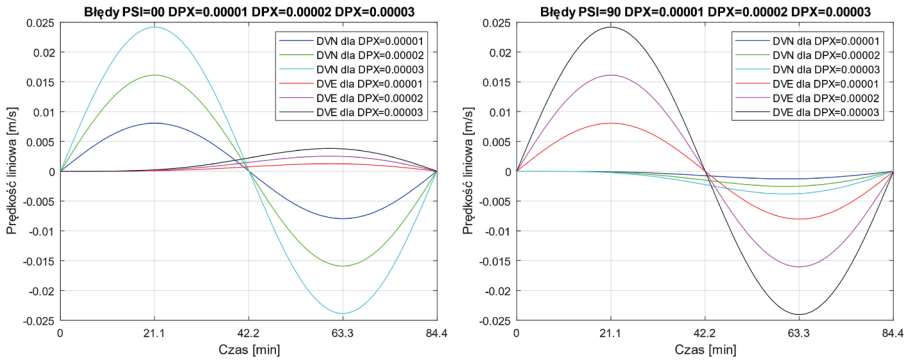

Fig. 5. Influence curves of the horizontal accelerometer error in the inclination channel for the course 0° (left) and 90° (right) for the baseline scheme (isolated errors only)

Source: P. Rogala, Statyczna Metoda Oceny..., op. cit.

To illustrate the impact of errors causing cosine travel speed errors [1-cos(ωS t)], modelling results (Figure 6) from the simulator are presented for selected DGX gyroscope error values in the longitudinal axis. The analysis showed that these errors only affect the eastern component of the velocity (0° heading) or the northern component (90° heading).

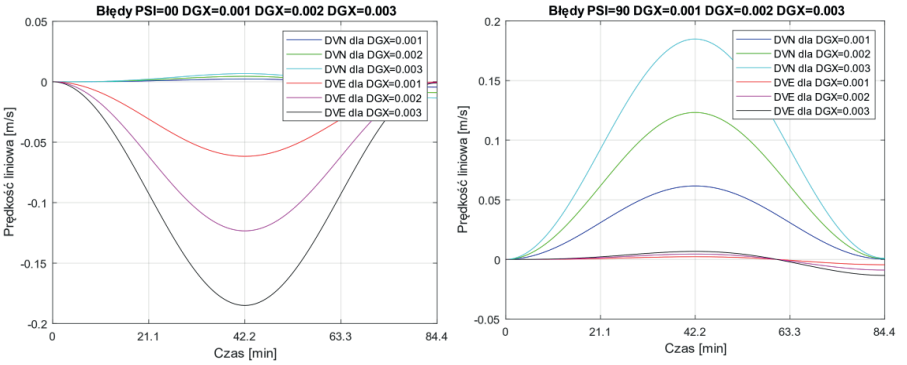

Fig. 6. Influence curves of the horizontal gyroscope error in the tilt channel for the 0° (left) and 90° (right) course for the baseline scheme (isolated errors only)

Source: P. Rogala, Statyczna Metoda Oceny..., op. cit.

 DOI: 10.55676/asi.v4i2.89

Simulation model tests ('cardanic' and 'non- cardanic') showed that the conditions of linearity and additivity of influence are met for the assumed changes in sensor errors and the levelling and gyrocompassing systems.

On the basis of simulation studies, the influence of individual isolated errors on the components of the travel speed was determined. The representative northern component of the travel speed for the analysis is presented as[19]:

$$\Delta V_N(t) = \left\{K_P^V\left[\Delta P_X\cos(\Psi)-\Delta P_Y\sin(\Psi)\right]+K_\Phi^V\left[\Delta\Theta\cos(\Psi)+\Delta\Phi\sin(\Psi)\right]\right\}\left[\sin(\omega_S t)\right]+$$
$$+\left\{K_G^V\left[\Delta G_X\sin(\Psi)+\Delta G_Y\cos(\Psi)\right]+K_\Psi^V\left[\Delta\Psi\cos(\Psi)\right]+K_\Omega^V\left[\Delta\varphi\sin(\Psi)\right]\right\}\left[1-\cos(\omega_S t)\right] \quad (6)$$

The error values of the travel speed components are best determined at characteristic points of the Schuler period. For 21.1 minutes, the maximum is reached by the error caused by the accelerometer error and levelling inaccuracy, and for 42.2 minutes by the gyroscope error and gyrocompass inaccuracy.

Taking the above into account, it is possible to compile a general matrix form of these relationships, presenting the error values of the individual components of the travel speed dependent on selected instrumental errors (interacting together or isolated).

$$\begin{bmatrix}\Delta V_N(21{,}1)\\ \Delta V_E(21{,}1)\\ \Delta V_N(42{,}2)\\ \Delta V_E(42{,}2)\\ \Delta V_N(63{,}3)\\ \Delta V_E(63{,}3)\\ \Delta V_N(105{,}5)\\ \Delta V_E(105{,}5)\end{bmatrix} = \begin{bmatrix}M_{11} & M_{12} & M_{13} & M_{14} & M_{15} & M_{16} & M_{17} & M_{18}\\ M_{21} & M_{22} & M_{23} & M_{24} & M_{25} & M_{26} & M_{27} & M_{28}\\ M_{31} & M_{32} & M_{33} & M_{34} & M_{35} & M_{36} & M_{37} & M_{38}\\ M_{41} & M_{42} & M_{43} & M_{44} & M_{45} & M_{46} & M_{47} & M_{48}\\ M_{51} & M_{52} & M_{53} & M_{54} & M_{55} & M_{56} & M_{57} & M_{58}\\ M_{61} & M_{62} & M_{63} & M_{64} & M_{65} & M_{66} & M_{67} & M_{68}\\ M_{71} & M_{72} & M_{73} & M_{74} & M_{75} & M_{76} & M_{77} & M_{78}\\ M_{81} & M_{82} & M_{83} & M_{84} & M_{85} & M_{86} & M_{87} & M_{88}\end{bmatrix} x \begin{bmatrix}\Delta P_X\\ \Delta P_Y\\ \Delta\Theta\\ \Delta\Phi\\ \Delta G_X\\ \Delta G_Y\\ \Delta\Psi\\ \Delta\varphi\end{bmatrix} \quad (7)$$

The values of the coefficients of the influence matrix of the individual instrumental errors on the components of the travel speed can be presented in tabular form:

806,00	0,00	137,80	0,00	0,00	61,60	-9,96	0,00
0,00	806,00	0,00	137,80	-61,60	0,00	0,00	12,80
0,00	0,00	0,00	0,00	0,00	123,20	-19,92	0,00
0,00	0,00	0,00	0,00	-123,20	0,00	0,00	25,60
-806,00	0,00	-137,80	0,00	0,00	61,60	-9,96	0,00
0,00	-806,00	0,00	-137,80	-61,60	0,00	0,00	12,80
569,84	0,00	97,42	0,00	0,00	105,15	-17,00	0,00
0,00	569,84	0,00	97,42	-105,15	0,00	0,00	21,85

A physical model of a gimbal-free inertial navigation system built at the Air Force Institute of Technology was used to verify the modelling results. The model is used to

[19] Ibidem.

develop a new version of the system and to diagnose systems on Polish Armed Forces aircraft (Su-22, MiG-29, F-16). Optimisation included hardware components and computational algorithms, as well as the presentation of input and output signals[20]. The model (Figure 7) uses FOG fibre optic sensors (0.01 deg/h error) and MEMS sensors (0.01 deg/s error).

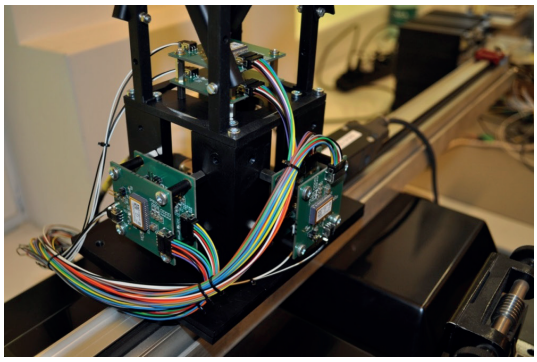

Fig. 7. View of the physical model of an inertial navigation system with MEMS sensors
Source: A. Szelmanowski et al., Optymalizacja Zbudowanego w ITWL..., op. cit.

The technical realisation of the physical model of the AHRS/INS class counting navigation system was made using modular technology with integrated STIM measurement elements[21]. The physical model of the system under construction was made to allow easy access to measurement signals through the use of a digital data bus and additional diagnostic and data imaging connectors on a laptop (with implemented algorithm) and oscilloscope.

The first optimization element was the MOS sensor module, containing algorithms for preliminary signal processing and spatial orientation. The next was the GMO computational module, the core of the system, with algorithms for calculating spatial orientation angles and the center of mass position. The final element was the communication and MKZ module, visualizing aircraft motion parameters and error calculations. The optimized MOS board[22] for MEMS accelerometers and FOG gyroscopes was built using FPGA systems for high data processing efficiency.

The main structure of the CPU1 application for the MOS module was created using STM32CubeIDE from STMicroelectronics, including the configuration of microcontroller interfaces according to the MOS board design. Optimization included identifying signal disturbances from sensors and developing a motion generation module to produce kinematic parameters of aircraft movement, set as constant or time-dependent values.

20 A. Szelmanowski et al., Optymalizacja Zbudowanego w ITWL..., op. cit.
21 Ibidem.
22 Ibidem.

 DOI: 10.55676/asi.v4i2.89

4. RESULTS OF TESTING THE INERTIAL NAVIGATION SYSTEM SIMULATOR

To verify the modeling results, a physical model of a strapdown inertial navigation system built at ITWL was used, along with systems from Su-22 aircraft and W-3PL helicopters. The AHRS/INS model includes communication modules SPI, RS-232, RS-485, ETHERNET, and MIL-1553B. As an educational simulator, it enables educational and training scenarios, the introduction of disturbances, and their impact analysis. It can also be used as a diagnostic simulator to verify real navigation systems[23]. The simulator allows testing various architectures and technological solutions in hardware and software, including sensor error models and advanced computational algorithms[24].

4.1. DEMONSTRATION AND TESTING OF THE NAVIGATION SYSTEM SIMULATOR INERTIAL

The built physical model of the inertial navigation system simulator with the STIM-800 measurement module was built on the KPA-5 rotating stand (Figure 8).

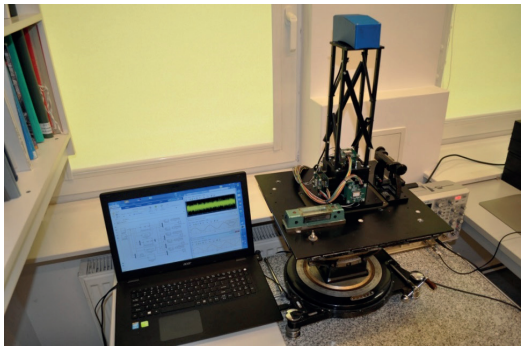

Fig. 8. View of the physical model of the inertial navigation system at the KPA-5 station
Source: A. Szelmanowski et al., Optymalizacja Zbudowanego w ITWL..., op. cit.

Preliminary testing of the simulator with the STIM-800 measurement module has made it possible to determine the noise level in the measurement signals of the accelerometers (Figure 9) and gyroscopes.

[23] A. Szelmanowski et al., Symulator Diagnostyczny..., op. cit.

[24] T.L. Grigorie, R.M. Botez, Modelling and Simulation Based Matlab/Simulink of a Strap-Down Inertial Navigation Systemów Errors Due to the Inertial Sensors, in Matlab Applications for the Practical Engineer, IntechOpen, 2014; Y.F. Jiang, Y.P. Lin, Error Analysis of Quaternion Transformations, IEEE Transactions of Aerospace and Electronic Systems 27, no. 4 (1991); H.K. Lee et al., Modeling Quaternion Error in SDINS: Computer Frame Approach, IEEE Transactions on Aerospace and Electronic Systems 34, no. 1, 1998; J.Z. Lai, P. Liv, L. Zhang, Coning Error Analysis and Compensation in Rotation Inertial Navigation System (in Chinese), Journal of Nanjing University of Aeronautics and Astronautics 2, 2012: 159–64.

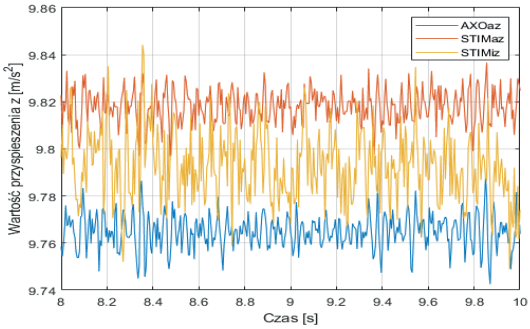

Fig. 9. The waveform of linear acceleration signals from STIM-318 at rest
Source: A. Szelmanowski et al., Symulator Diagnostyczny..., op. cit.

4.2. INERTIAL NAVIGATION SYSTEM FAULT DIAGNOSIS AND ANALYSIS

The test results of the inertial navigation system simulator were used to diagnose the technical condition of real inertial navigation systems operated in the aviation of the Polish Armed Forces. The tests were conducted for a gimballed system (using the IKW-8 system installed on Su-22 aircraft as an example) and a non-cardaned system (using the EGI-3000 system installed on Su-22 aircraft as an example). (based on the EGI-3000 system installed on W-3PL helicopters).

Studies of the course of travel speed determination errors in the IKW-8 system were carried out in static conditions, during which the gimbal measuring platform was built from the deck of a Su-22 aircraft and placed on a KPA-5 tilt table, allowing the set angles of roll, pitch and heading to be set (Figure 10).

Fig. 10. View of the IKW-8 inertial navigation system on stand KPA-5
Source: P. Rogala, Statyczna Metoda Oceny..., op. cit.

 DOI: 10.55676/asi.v4i2.89

The U1 indicator on the PNK-3M desktop[25] was used to measure the waveforms of the travel speed components determined by the IKW-8 system. The selection of the appropriate IKW-8 system transmitters connected to the U1 indicator is provided by multi-position switch W2. The plot value of the U1 indicator is 2 angular minutes and allows angular values to be read with an accuracy of 1 angular minute.

An example of the error waveform of the northern component of the travelling speed of the IKW-8 system for one Schuler period (Figure 11) showed that the dominant influences are the instrumental errors of the accelerometers (for which the DHN coefficient of the curve according to the function $\sin(\omega_s \cdot t)$ is equal: -3.055 m/s), while less influenced by gyroscopic errors (for which the DAN coefficient of the curve according to function $[1-\cos(\omega_s \cdot t)]$ is equal: -0.893 m/s).

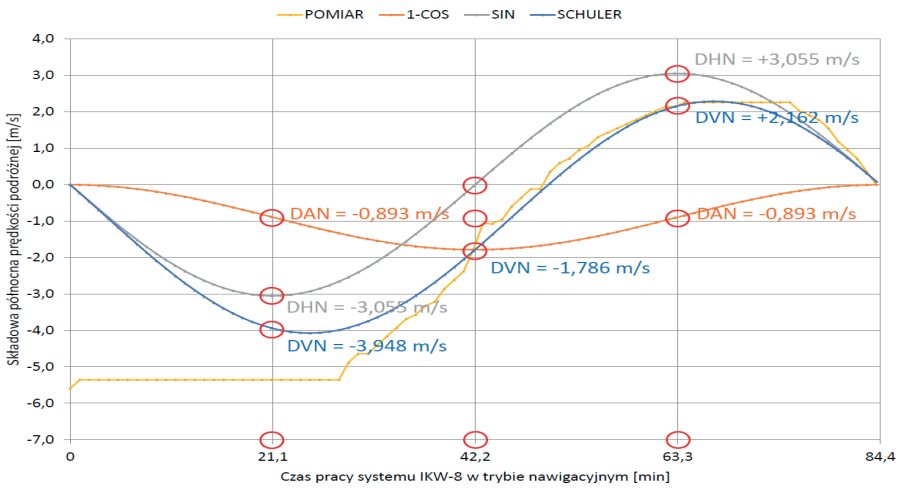

Fig. 11. Error waveforms of the northern component of the IKW-8 system travel speed
Source: P. Rogala, Statyczna Metoda Oceny..., op. cit.

Investigations into the course of travel speed determination errors in the EGI-3000 system were carried out in static conditions, during which a cardan-free measuring platform was built from a W-3PL helicopter and placed on a KPA-5 tilt table, allowing the setting of the preset roll, pitch and heading angles (Figure 12). A MIL-1553B digital data bus monitor was used to read out the values of the travel speed components, allowing the parameters determined by this system to be recorded.

[25] P. Rogala, Statyczna Metoda Oceny..., op. cit.

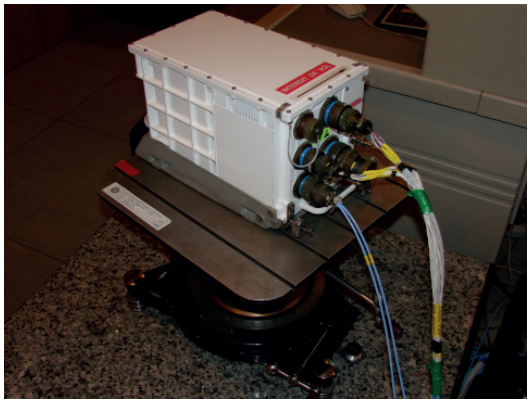

Fig. 12. View of the EGI-3000 inertial navigation system on stand KPA-5
Source: P. Rogala, Statyczna Metoda Oceny..., op. cit.

An example of the error waveform of the northern component of the travel speed of the EGI-3000 system for one Schuler period (Figure 13) showed that the dominant influences are the instrumental errors of the gyroscopes (for which the DAN coefficient of the curve according to function $[1-\cos(\omega_s \cdot t)]$ is equal: +0.314 m/s), while less influential are the errors of the accelerometers (for which the DHN coefficient of the curve according to the function $\sin(\omega_s \cdot t)$ is equal -0.089 m/s).

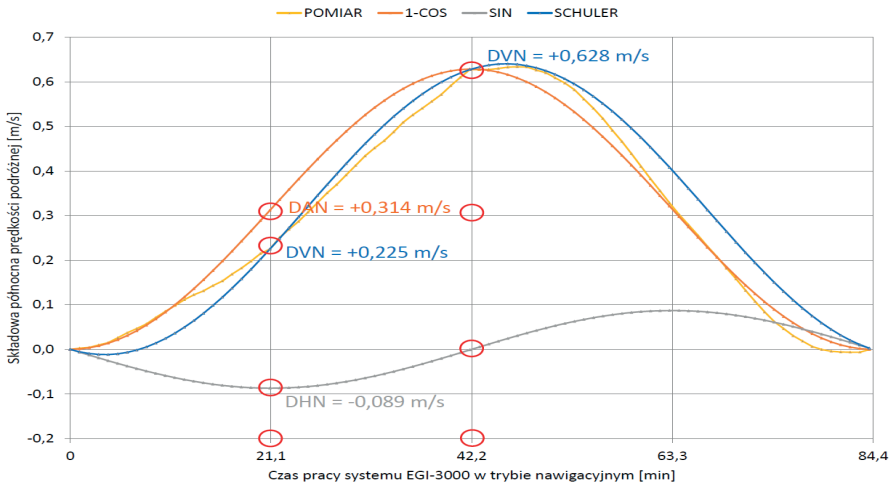

Fig. 13. Error waveform of the northern component of the travel speed of the EGI-3000 system
Source: P. Rogala, Statyczna Metoda Oceny..., op. cit.

 DOI: 10.55676/asi.v4i2.89

The analysis of waveforms for the northern and eastern travel speed components allowed approximation using verified mathematical relations, considering the Schuler frequency. This enabled further analysis and determination of error values at selected times during the Schuler period.

Repeated error measurements of the IKW-8 and EGI-3000 systems confirmed their oscillatory nature due to the Schuler pendulum and the non-repeatability of results. For the IKW-8 system, maximum travel speed errors reached ±30 m/s, within the ±50 m/s limit. For the EGI-3000 system, errors reached ±0.6 m/s, within the ±0.7 m/s limit.

5. CONCLUSIONS

Inertial navigation systems are now the primary source of navigational information used on board modern aircraft. It is particularly important to obtain knowledge of inertial navigation system errors in the determination of navigational position, travel speed and spatial orientation angles, as well as the conditions under which they occur and the possibility of correction.

One of the main problems undertaken in this work is to determine the possibility of estimating the errors of the inertial navigation system in relation to the instrumental errors of the applied motion sensors in inertial space (accelerometers and angular velocity sensors) and the levelling and gyrocompassing systems. The method of analysing the travel speed waveforms and the results of error identification are presented on the example of a cardan system (IKW-8) and a non-cardan system (EGI-3000).

The main achievement presented in the paper is the developed mathematical model, which allows for the determination of the values of errors in the components of travel speed and navigational position in selected moments of time of the inertial navigation system. The model makes it possible to determine the impact of individual instrumental errors of the system interacting individually (isolated errors) as well as occurring jointly.

The presented scope of optimisation of the physical model of the inertial navigation system built at ITWL included the improvement of the hardware layer and operation algorithms, as well as the possibility of modelling the operation with particular emphasis on the module of input signals from linear acceleration and angular velocity sensors for the aircraft as an object with spatial motion.

The built simulator of the inertial navigation system may find application in education, for familiarisation of students and lecturers of avionics faculties of technical universities, and for training of engineering and aviation service personnel and experts of state aviation accident investigation committees.

The foreseen research direction is the construction and implementation of a diagnostic simulator for the detection and identification of inertial navigation system malfunctions in relation to the main instrumental errors (accelerometers and gyroscopes). An

interesting task is the use of new technologies in the construction of inertial sensors and optimal computational algorithms using artificial intelligence.

BIBLIOGRAPHY

Godha S., Lachapelle G., Foot Mounted Inertial System for Pedestrian Navigation. Measurement Science and Technology 19, no. 7 (May 2008): 075202. https://doi.org/10.1088/0957-0233/19/7/075202.

Gosiewski Z., Ortyl A., Algorytmy Inercjalnego Bezkardanowego Systemu Orientacji i Położenia Obiektu o Ruchu Przestrzennym. Vol. 12. Awionika. Wyd. Instytutu Lotnictwa, Warszawa 1999.

Grigorie T.L., Botez R.M., Modelling and Simulation Based Matlab/Simulink of a Strap-Down Inertial Navigation Systemów Errors Due to the Inertial Sensors. In Matlab Applications for the Practical Engineer. IntechOpen, 2014.

Izdebski M., Jacyna-Gołda I., Gołda P., Minimisation of the Probability of Serious Road Accidents in the Transport of Dangerous Goods. Reliability Engineering & System Safety 217 (2022): 108093.

Jiang Y.F., Lin Y.P., Error Analysis of Quaternion Transformations. IEEE Transactions of Aerospace and Electronic Systems 27, no. 4 (1991).

Kayton M., Fried W.R., Avionics Navigation Systems. 2nd Edition. A Wiley-Interscience Publication, 1997.

Lai J.Z., Liv P., Zhang L., Coning Error Analysis and Compensation in Rotation Inertial Navigation System (in Chinese). Journal of Nanjing University of Aeronautics and Astronautics 2 (2012): 159–64.

Lee H.K., Lee J.G., Roh Y.K., ParkC.G., Modeling Quaternion Error in SDINS: Computer Frame Approach. IEEE Transactions on Aerospace and Electronic Systems 34, no. 1 (1998).

Mytych J., Ligarski M.J., Expert Assessment of Conditions for Accredited Quality Management System Functioning in Testing Laboratories. Management Systems in Production Engineering 26, no. 1 (March 1, 2018): 42–48. https://doi.org/10.2478/mspe-2018-0007.

Rogala P., Statyczna Metoda Oceny Stanu Technicznego Systemu Nawigacji Inercjalnej. ITWL, 2023.

Savage P.G., Strapdown Inertial Navigation Integration Algorithm Design Part 1, Attitude Algorithms. Journal of Guidance, Control and Dynamics 21, no. 1 (1998).

Szelmanowski A., Borowski J., Poświata J., Rogala P., Symulator Diagnostyczny Dla Systemu Nawigacji Inercjalnej Wykorzystujący Statyczną Metodę Oceny Stanu Technicznego. In XI Konferencja Naukowa Bezpieczeństwa i Niezawodności KONBiN 2022, 07-10.06. Piekary Śląskie 2022.

Szelmanowski A., Michalak S., Borowski J., Cieślik A., Poświata J., Michałowski P., Kajewski P., Jaruga S., Chybowski M., Optymalizacja Zbudowanego w ITWL Modelu

 DOI: 10.55676/asi.v4i2.89

Fizycznego Systemu Nawigacji Zliczeniowej Klasy AHRS/INS w Zakresie Jego Konfiguracji Sprzętowej i Algorytmów Działania. BT ITWL, Warszawa 2021.

THALES, Functional Specification of Inertial Navigation System TOTEM-3000 / EGI-3000. Bordeaux, France 2010.

Yang Y., Song Y., Zhu Y., Innovation Research on Strapdown Inertial Navigation Technology. International Journal of Mechatronics and Applied Mechanics 2017 (January 1, 2017): 72–77.

Zieja M., Wawrzyński W., Tomaszewska J., Sigiel N., A Method for the Interpretation of Sonar Data Recorded during Autonomous Underwater Vehicle Missions. Polish Maritime Research 29, no. 3 (September 1, 2022): 176–86. https://doi.org/10.2478/pomr-2022-0038.